NJC

New Journal of Chemistry

A journal for new directions in chemistry

Accepted Manuscript

This article can be cited before page numbers have been issued, to do this please use: J. Wang, S. Wei, T. Li, L. Xing, M. Cao, N. Jiang, M. Guo, D. Zuo and X. Zhai, *New J. Chem.*, 2020, DOI: 10.1039/C9NJ05980F.

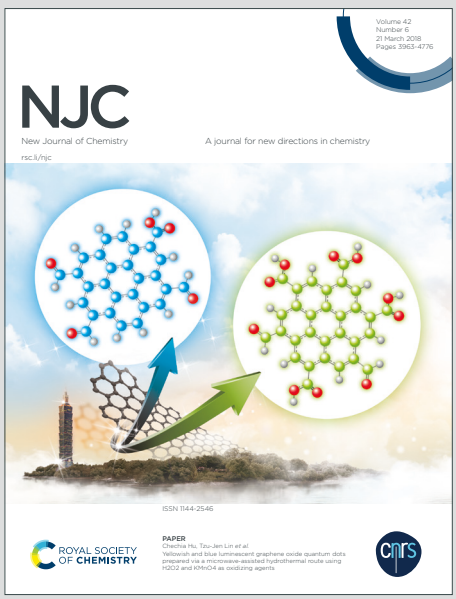

This is an Accepted Manuscript, which has been through the Royal Society of Chemistry peer review process and has been accepted for publication.

Accepted Manuscripts are published online shortly after acceptance, before technical editing, formatting and proof reading. Using this free service, authors can make their results available to the community, in citable form, before we publish the edited article. We will replace this Accepted Manuscript with the edited and formatted Advance Article as soon as it is available.

You can find more information about Accepted Manuscripts in the Information for Authors.

Please note that technical editing may introduce minor changes to the text and/or graphics, which may alter content. The journal's standard Terms & Conditions and the Ethical guidelines still apply. In no event shall the Royal Society of Chemistry be held responsible for any errors or omissions in this Accepted Manuscript or any consequences arising from the use of any information it contains.

View Article Online
DOI: 10.1039/C9NJ05980F

Structure-based design of 2,4-diaminopyrimidine derivatives bearing pyrrolyl group as ALK & ROS1 inhibitors

Jie Wang[a], Shangfei Wei[a], Tong Li[a], Lingyun Xing [a], Meng Cao[a], Nan Jiang[a], Ming Guo[a], Daiying Zuo[b, *], Xin Zhai[a,*]

[a] Key Laboratory of Structure-Based Drug Design and Discovery, Ministry of Education, Shenyang Pharmaceutical University, Shenyang 110016, PR China

[b] Department of Pharmacology, Shenyang Pharmaceutical University, Shenyang 110016, China.

*Corresponding author.

E-mail address: zhaixin_syphu@126.com (Xin Zhai), zuodaiying@163.com (Daiying. Zuo).

Abstract:

In order to develop potent ALK and ROS1 dual inhibitors, twenty-eight 2,4-diaminopyrimidine derivatives (**9a-9n** and **10a-10n**) bearing pyrrolyl moiety were designed and synthesized based on co-crystal structure of ceritinib with ALK^{wt} protein. Most compounds displayed considerable activity against ALK and ROS1 addicted cells, meanwhile, compound **10d** showed excellent activity against Karpas299, H2228 and HCC78 with IC_{50} values of 0.01, 0.08 and 0.042 μM. Subsequently, seven compounds were selected for kinase studies *in vitro*, resulting in the discovery of **10d** with IC_{50} values of 1.8, 4.3 and 3.6 nM against ALK, ALK^{L1196M} and ROS1, respectively. Furthermore, the biological assays revealed that compound **10d** induced cell apoptosis in a dose-dependent manner. Ultimately, molecular docking studies presented the reasonable and optimal binding interactions with ALK^{wt} and ROS1.

Keywords: synthesis; 2,4-diaminopyrimidine; ALK&ROS1; anti-proliferation activities

View Article Online
DOI: 10.1039/C9NJ05980F

1. Introduction

Anaplastic lymphoma kinase (ALK) receptor tyrosine kinase and its ligand have received extensive attention recently among the target-based therapy.[1] In contrast to dormancy in normal tissues, abnormal ALK gene in a variety of tumor cells was mainly represented by gene fusion,[2] overexpression and point mutation.[3] Moreover, the transforming echinoderm microtubule associated protein like 4-ALK (EML4-ALK) fusion gene was recognized as the driver gene for non-small cell lung cancer (NSCLC).[4] Similar to ALK, c-ros oncogene 1 (ROS1), an orphan receptor tyrosine kinase, has been identified in the expression of oncogenic fusion proteins in a subset of NSCLC patients.[5-6] Based on approximately 49% amino acid homology of ALK and ROS1,[7] a majority of ALK inhibitors had shown outstanding efficacy in ROS1 positive NSCLC patients, greatly accelerating the clinical development of ALK and ROS1 dual inhibitors.[8]

Crizotinib was the first ALK and ROS1 dual inhibitor approved in 2011 based on the impressive objective response rate and progression-free survival times as the standard therapy for ALK-positive lung cancer patients.[9-10] However, resistance to crizotinib was tested in patients within about 1 year of treatment, which exhibited tumor relapse and regrowth.[11-12] As a consequence, several crizotinib-resistant ALK inhibitors have been reported, including ceritinib,[13] alectinib,[14] brigatinib,[15] lorlatinib[16] and TPX-00L05 [17] (**Fig. 1**).

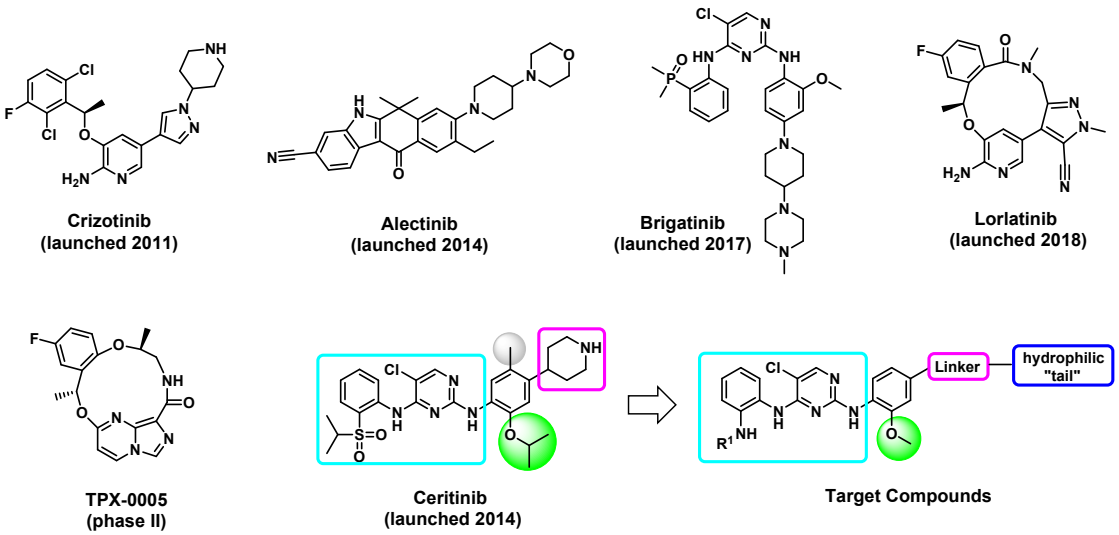

Fig. 1 Structures of ALK inhibitors and design strategies of target compounds.

The co-crystal structure of ceritinib with ALK^{wt} (**Fig. 2A**)[18-19] indicated that ceritinib as the lead compound embedded the surface of ALK protein completely, meanwhile, the key fragments of 2,4-diarylaminopyrimidine and 5-Cl atom were retained to assume the kinase hinge binding moiety and the essential protein interactions in the ATP binding site.[20] Then, for the sake of improving the potency and diversity, primary structural modification was mainly focused on the optimization

View Article Online
DOI: 10.1039/C9NJ05980F

of aromatic group substituents. [21] As shown in **Fig. 2B** and **2C**, the isopropyl sulfonyl motif could form important hydrogen and hydrophobic effect, therefore, sulfonamido and acetamido segments were chosen to guarantee or even enrich the interaction manners.[22-23] In term of the effect of steric hindrance, methoxyl group was disclosed as an effective isopropoxyl surrogate.[24]

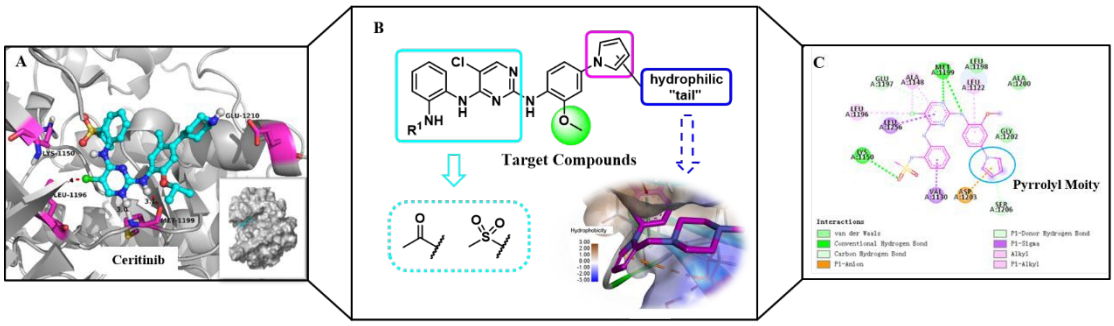

Fig. 2 Design strategy for target compounds based on co-crystal structure of ceritinib with ALK^{wt} (PDB ID code: 4MKC). (A) Binding conformation of ceritinib (blue sticks) in the ATP binding site of ALK^{wt} and the existence of ceritinib on the surface of ALK^{wt} protein. (B) The general structural formula of target compounds and hydrophobic diagram of the "tail". (C) 2D diagram of the interaction between pyrrolyl moiety and ALK^{wt}.

Recently, extensive biological activities such as anti-ulcer,[25] antitumor [26] and anti-inflammatory [27] of pyrrolyl-containing compounds have received the consideration in the field of drug design and development. As expected, 2D diagram (**Fig. 2C**) showed that the pyrrolyl fragment formed new π-anion and carbon hydrogen bond interactions, indicating the introduction of pyrrolyl moiety was considerable to improve the structural optimization. Thus, pyrrolyl segment was accessed as a linker to improve the affinity with the biological target. On the other hand, simulation hydrophobic diagram of the "tail" revealed that hydrophilic "tail" was located in a strong hydrophilic region. For further verification, different aliphatic and alicyclic amines would be brought to discuss the influence of hydrophilic moieties in solvent-interaction region.[28]

Accordingly, twenty-eight 2,4-diaminopyrimidine compounds were subjected to design, synthesis and prediction for their physical properties, followed by their anti-proliferative activities *in vitro* assay against five human cancer cell lines to study the structure-activity relationships. In addition, seven compounds were further evaluated for their activity towards the ALK, ALK^{L1196M}, ROS1 and EGFR kinase *in vitro*. Especially, the cell apoptosis assay and molecular docking mode analysis of the most potent compound **10d** were also performed.

2. Chemistry

Target compounds **9a-9n** and **10a-10n** were synthesized as illustrated in **Scheme 1**. Substitution of commercially available 2,4,5-trichloropyrimidine (**1**) with bnzene-1,2-diamine (**2**) afforded intermediate **3**, which was acylated by acetyl chloride or methanesulfonyl chloride in the presence of triethylamine without further

purification to bring the key intermediates **4a** and **4b** in high yields.[29] Meanwhile, treatment of 4-fluoro-2-methoxy-1-nitrobenzene (**5**) with 1*H*-pyrrole (**6**) in DMF at 100 °C for 8 h gave rise to **7** as a yellow solid. Refluxing in ethanol, the intermediate **8** was obtained *via* reduction of compound **7** with iron powder and catalytic amounts of ammonium chloride.[30] Subsequently, **4a** and **4b** were reacted with **8** in refluxing isopropanol and purified on the silica gel column to arrive at critical compounds **9a** and **10a**. Eventually, Mannich reaction of the resultant **9a** and **10a** with appropriate aliphatic amines and 37% formaldehyde in the presence of acetic acid at room temperature provided target compounds **9b-9n** and **10b-10n** in satisfied yields.

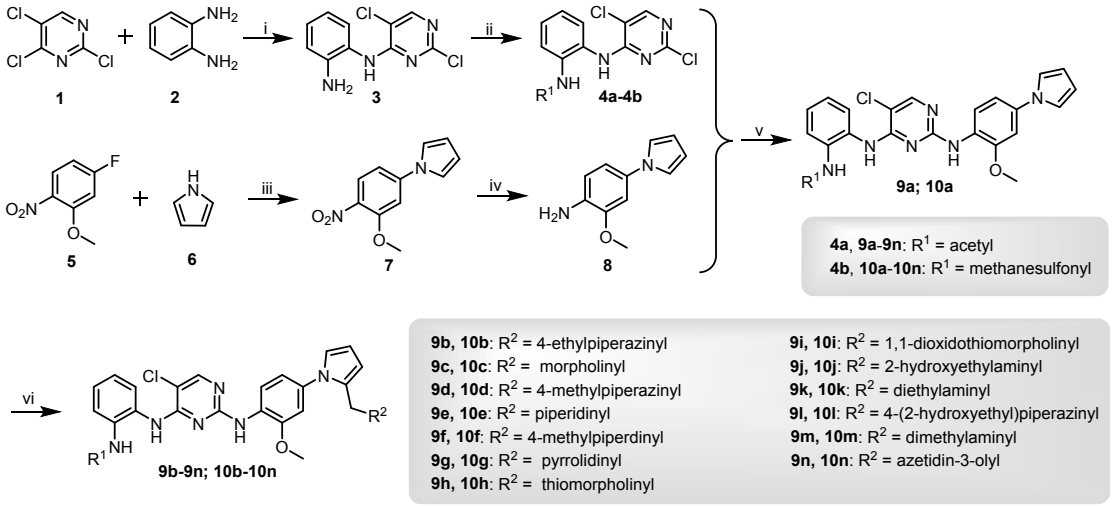

Scheme 1. Reagents and conditions: (i) DIPEA, isopropanol, 80 °C; (ii) the acyl chloride of R^1, TEA, DCM, rt; (iii) K_2CO_3, DMF, 100 °C; (iv) iron powder, hydrochloric acid, ethanol/water (9:1), 80 °C; (v) IPA, 80 °C; (vi) aliphatic amines, acetic acid, formaldehyde (37%), rt.

3. Results and discussion

3.1. Physical properties, in vitro anti-proliferative activity and SARs study

The physical properties were listed to assess the "drug-likeness" of compounds **9a-9n** and **10a-10n** according to the Lipinski rule.[31] The predicted results of cLogP and TPSA were shown in **Table 1**. The lipophilic quantity cLogP is the logarithm of the partition coefficient between 1-octanol and water and the topological polar surface area (TPSA) is defined as the surface sum over all polar atoms for the optimisation of cell permeability. Most compounds with cLogP of less than 5 and TPSA of less than 140 Å² revealed the better druggability which were essential to execute further *in vitro* assays.

Table 1. Physical properties of **9a-9n** and **10a-10n**.

Compd.	[a] cLogP	[b] TPSA (Å²)	Compd.	cLogP	TPSA (Å²)
9a	3.75	93.10	**10a**	3.36	118.55
9b	3.81	99.58	**10b**	3.43	125.03
9c	3.56	105.57	**10c**	3.19	131.02

9d	3.53	99.58	**10d**	3.20	125.03
9e	4.41	96.34	**10e**	3.99	121.79
9f	4.67	96.34	**10f**	4.33	121.79
9g	4.14	96.34	**10g**	3.73	121.79
9h	4.12	121.64	**10h**	3.65	147.09
9i	3.31	138.86	**10i**	2.92	164.31
9j	3.08	125.36	**10j**	2.63	150.81
9k	4.35	96.34	**10k**	3.97	121.79
9l	3.08	119.81	**10l**	2.68	145.26
9m	3.79	96.34	**10m**	3.20	121.79
9n	3.06	116.57	**10n**	2.59	142.02
[c]**Ceritinib**	5.62	113.62	**Ceritinib**	5.62	113.62

[a] [c]LogP measured between 1-octanol/water phosphate buffered.

[b] TPSA defined the surface sum over all polar atoms.

[c] Used as positive control.

The MTT assay *in vitro* was adopted to evaluate the anti-proliferation activities of all the synthesized compounds **9a-9n** and **10a-10n**. Taking ceritinib as the positive control, target compounds were investigated the potency against NPM-ALK-addicted Karpas299 (Human anaplastic large cell lymphoma cell line) cell, EML4-ALK-addicted H2228 (Human non-small-cell lung cancer cell line) cell and ROS1-addicted HCC78 (Human lung adenocarcinoma cell line) cell as well as the off-target cells, namely H460 (Human large cell lung cancer cell line) and A549 (Human EGFR-positive non-small-cell lung cancer cell line). The results of IC_{50} values were shown in **Table 2**, as mean values of experiments performed in triplicate.

As illustrated in **Table 2**, satisfactory data were obtained that most compounds exhibited moderate to excellent cytotoxic activity and marked selectivity. As a general trend, the title compounds showed more potent on Karpas299, H2228 and HCC78 cells superior to H460 and A549 cell lines. Moreover, introduction of hydrophilic group bending down into the solvent area displayed higher anti-proliferation activities compared to compounds **9a** and **10a.** Among target compounds, the most promising compound **10d** showed excellent activity against Karpas299, H2228 and HCC78 with the IC_{50} values of 0.01, 0.08 and 0.042 μM, which were 2.7-, 1.2- and 1.8-fold more active than ceritinib (0.027, 0.099 and 0.074 μM).

The initial SARs study was commenced by the introduction of diverse R^1 at the "head" of the benzene ring. It was worth noting that sulfonamido group compounds **10a-10n** turned out to significantly enhance the potency as compared with compounds **9a-9n** bearing acetamido, suggesting that sulfonamido group was necessary to the anti-proliferation effect. Among the target-addicted cells, most of the compounds showed similar activity trends.

Further analysis revealed that different hydrophilic R^2 had a systematic influence on their potency. Compounds **9i** and **10i** bearing 1,1-dioxidothiomorpholinyl moiety showed decreased or even vanished activity with IC_{50} of more than 1 μM against Karpas299, H2228 and HCC78. The loss in activity might be due to the steric clash. Notably, the same trend was observed among compounds **10k** bearing diethylaminyl and **10m** bearing dimethylaminyl. Interestingly, in Karpas299 cells, mono-substituted compounds **9j** (IC_{50} = 0.23 μM) and **10j** (IC_{50} = 0.09 μM) displayed moderate potency as compared to other compounds bearing double-substituted group. Meanwhile, in H2228 cells, the morpholinyl **10c** (IC_{50} = 0.37 μM) and 4-methylpiperazinyl **10d** (IC_{50} = 0.08 μM) afforded greater activity towards piperidinyl **10e** (IC_{50} = 0.55 μM) and 4-methylpiperdinyl **10f** (IC_{50} = 0.64 μM), indicating the embedded of electron-withdrawing group was advantageous to potency. In addition, incorporation of a polar moiety (hydroxyl group) on **10b** gave rise to compound **10l** which achieved 2.1-, 1.1- and 1.7-fold activities against Karpas299, H2228 and HCC78 cell lines, respectively.

Table 2. Cytotoxicity of **9a-9n** and **10a-10n** against Karpas299, H2228, HCC78, H460 and A549 cell lines *in vitro*.

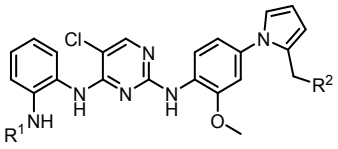

Compd.	R^1	R^2	[a]IC_{50} (μM) ± SD				
			Karpas299	H2228	HCC78	H460	A549
9a		-	0.56±0.02	1.01±0.31	0.83±0.12	0.59±0.25	0.48±0.07
9b		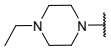	0.48±0.06	0.54±0.022	0.72±0.08	1.77±0.43	>10
9c			0.51±0.018	0.86±0.013	0.89±0.06	2.58±0.67	1.38±0.02
9d			0.046±0.001	0.12±0.006	0.13±0.01	1.37±0.47	1.98±0.09
9e			0.60±0.021	0.81±0.04	0.66±0.08	2.3±0.39	1.69±0.22
9f			0.42±0.005	0.59±0.012	0.54±0.03	1.54±0.25	0.75±0.04
9g			0.71±0.007	0.78±0.03	1.03±0.18	1.23±0.47	5.47±0.34
9h			0.86±0.004	1.82±0.40	1.74±0.35	0.80±0.09	6.17±0.21

View Article Online
DOI: 10.1039/C9NJ05980F

Compd.	R^1	R^2	$^aIC_{50}$ (μM) ± SD				
			Karpas299	H2228	HCC78	H460	A549
9i			1.23±0.05	4.31±0.72	3.46±0.18	1.01±0.03	3.46±0.23
9j		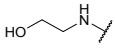	0.24±0.08	0.60±0.34	0.27±0.02	1.08±0.07	3.56±0.39
9k			0.62±0.09	1.06±0.04	0.92±0.08	0.12±0.01	0.93±0.24
9l		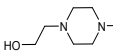	0.26±0.01	0.84±0.06	0.78±0.04	4.22±0.28	0.78±0.02
9m			0.18±0.041	0.37±0.08	0.43±0.06	0.68±0.16	2.11±0.31
9n			0.36±0.04	0.66±0.07	0.63±0.03	4.19±0.45	3.86±0.09
10a		-	0.16±0.04	0.71±0.07	0.51±0.11	0.13±0.03	2.62±0.09
10b		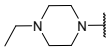	0.18±0.01	0.24±0.02	0.44±0.03	3.38±0.03	1.20±0.07
10c			0.14±0.03	0.37±0.06	0.36±0.08	2.68±0.04	3.41±0.03
10d			0.01±0.006	0.08±0.003	0.042±0.01	2.50±0.06	1.09±0.08
10e			0.20±0.02	0.55±0.09	0.48±0.02	2.67±0.02	1.56±0.23
10f			0.32±0.03	0.64±0.01	0.31±0.04	3.10±0.05	2.96±0.68
10g			0.36±0.04	0.70±0.013	0.22±0.01	1.63±0.18	3.4±0.06
10h			0.44±0.017	1.29±0.21	0.82±0.13	1.41±0.33	2.26±0.09
10i			1.04±0.16	3.21±0.73	1.87±0.21	>10	7.00±1.04

View Article Online
DOI: 10.1039/C9NJ05980F

Compd.	R^1	R^2	$^aIC_{50}$ (μM) ± SD				
			Karpas299	H2228	HCC78	H460	A549
10j		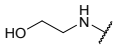	0.09±0.008	0.27±0.06	0.093±0.02	1.87±0.05	1.56±0.07
10k			0.23±0.005	0.50±0.07	0.29±0.04	2.91±0.30	0.71±0.03
10l		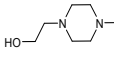	0.084±0.009	0.21±0.03	0.26±0.021	0.44±0.04	0.94±0.08
10m			0.059±0.004	0.18±0.05	0.12±0.07	3.12±0.24	1.21±0.25
10n			0.12±0.008	0.36±0.02	0.18±0.03	1.28±0.42	1.05±0.16
[b]**Ceritinib**			0.027±0.002	0.099±0.01	0.074±0.01	0.20±0.03	0.79±0.07

[a] Data presented is mean ± SD value of three independent experiments.
[b] Used as positive control.

3.2. In vitro enzymatic assays

In view of the promising activity of target compounds on ALK and ROS1 addicted cells, seven optimized compounds were selected for further molecular-level studies with ALK, ALK^{L1196M}, ROS1 and EGFR kinases *in vitro*. The non-related EGFR kinase was selected to verify the kinase selectivity. Taking ceritinib as the positive control, the results expressed as IC_{50} were summarized in **Table 3**.

As illustrated in **Table 3**, most compounds (**9d**, **10b**, **10d** and **10m**) performed potent inhibitory activities against ALK, ALK^{L1196M} and ROS1 as dual kinases inhibitors with IC_{50} below 30 nM, parallelled to the cellular activity. Contrastly, compound **9i** bearing acetamido (R^1) and thiomorpholine 1,1-dioxide (R^2) fragment (IC_{50} > 100 nM) extinguished the activity dramatically. Additionally, both tested compounds and ceritinib revealed no activity against EGFR with IC_{50} value over 100 nM. To our delight, compound **10d** was distinguished with IC_{50} value of 1.8, 4.3 and 3.6 nM against ALK, ALK^{L1196M} and ROS1 which was comparable to that of ceritinib (IC_{50} = 2.3, 8.9 and 2.7 nM). Thus, compound **10d** was preferred for further evaluation in forthcoming biological and molecular docking studies.

Table 3. Enzymatic inhibition of selected compounds **9d**, **9i**, **9l**, **10b**, **10d**, **10g** and **10m** against ALK, ALK^{L1196M}, ROS1 and EGFR *in vitro*.

Compd.	IC_{50} (nM)			
	ALK	ALK^{L1196M}	ROS1	EGFR
9d	4.5	9.4	4.1	>100
9i	>100	>100	>100	>100
9l	16.2	28.9	23.6	>100

View Article Online
DOI: 10.1039/C9NJ05980F

10b	7.2	9.0	6.3	>100
10d	1.8	4.3	3.6	>100
10g	7.4	18.2	9.2	>100
10m	28	7.8	5.6	>100
[a]**Ceritinib**	2.3	8.9	2.7	>100

[a] Used as positive control.

3.3. Apoptosis analysis

To further determine the promising anti-proliferation potency, compound **10d** was monitored the apoptotic morphological changes with Hoechst 33258 or AO/EB staining for 48 h in Karpas299 cells; ceritinib was tested for comparison.[32]

As shown in the upper part in **Fig. 3**, control cells group showed uniform blue fluorescence by Hoechst 33258 staining. Nuclear shrinkage and fragmentation were performed on **10d** or ceritinib treated cells. Meanwhile, the number and degree of apoptosis cells were increased obviously on **10d** of 50 nM treatment group. As shown in the lower part in **Fig. 3**, control cells group showed homogeneous green fluorescence and normal structure by AO/EB staining. At the concentration of 25 nM, **10d** or ceritinib treated cells increased the number of early apoptosis cells with enhanced green fluorescence. Moreover, the terminal apoptosis cells accompanied by the emergence of irregular orange-red fluorescence were increased markedly on **10d** of 50 nM treatment group. In terms of the similar phenomena observed in Hoechst 33258 or AO/EB staining, **10d** was revealed to promote Karpas299 cell apoptosis in a dose-dependent manner.

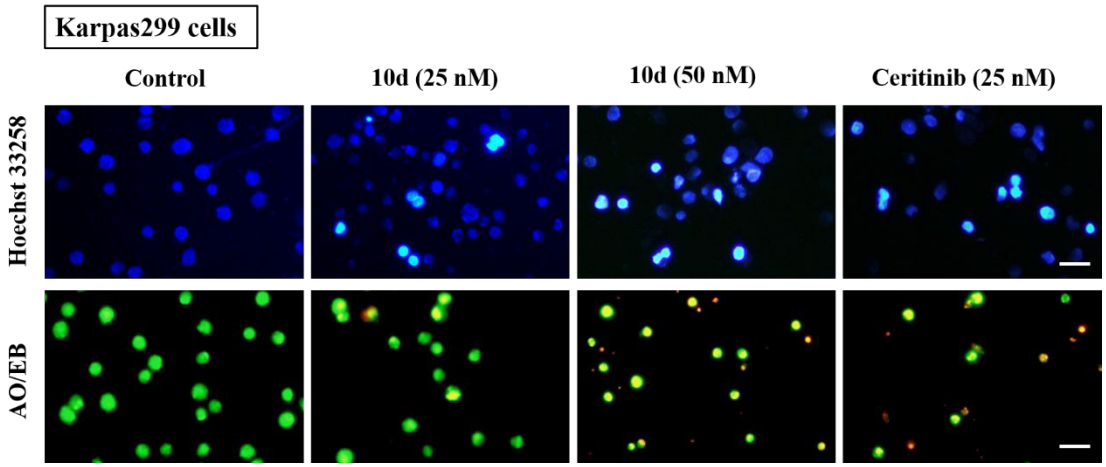

Fig. 3 10d induces apoptosis in Karpas299 cells. Karpas299 cells were treated with **10d** (25 and 50 nM) or ceritinib (25 nM) for 24 h, then stained with Hoechst 33258 or AO/EB and examined by fluorescence microscope.

3.4. Molecular docking studies

Simulating molecular dockings could comprehend the binding pattern between ligand and protein intuitively. Based on the co-crystal structure of ceritinib with ALK^{wt} (PDB ID code: 4MKC) [19] and ROS1 (PDB ID code: 3ZBF),[33] the

conformations were conducted using Pymol and the 2D binding modes were generated from Discovery Studio 2017 (**Fig. 4**).

Structural comparisons in **Fig. 4A** exhibited that **10d** and ceritinib occupied the same active site as expected. From the 2D diagram of **Fig. 4B** and **4D**, the structural domain of 5-chloro-2,4-diaminopyrimidine skeleton formed hydrogen bond with Met1199, hydrophobic interaction with Leu1196 and linked up to Val1130 and Leu1256 by aryl interactions. Moreover, **10d** containing pyrrolyl group increased the effect of π-anion interaction with Asp1203. Compared with **9d** bearing acetamido group (**Fig. 4E**), the sulfonamido compound **10d** engaged a new hydrogen bond onto the backbone nitrogen of Lys1150.

As demonstrated in **Fig. 4F**, the main binding driving force was thought to be matching between **10d** and ROS1. Concretely, **10d** was involved in the hydrophobic interactions with Ala1978, Val1959, Leu2026 and Lys1980. In particular, the pyrimidine and 4-NH formed hydrogen interaction with Met2029, as might be the reason that **10d** could enhance the ROS1 enzyme activity. Thus, the results from the docking study revealed that compound **10d** was in accordance with the SARs analysis as an ALK and ROS1 inhibitor.

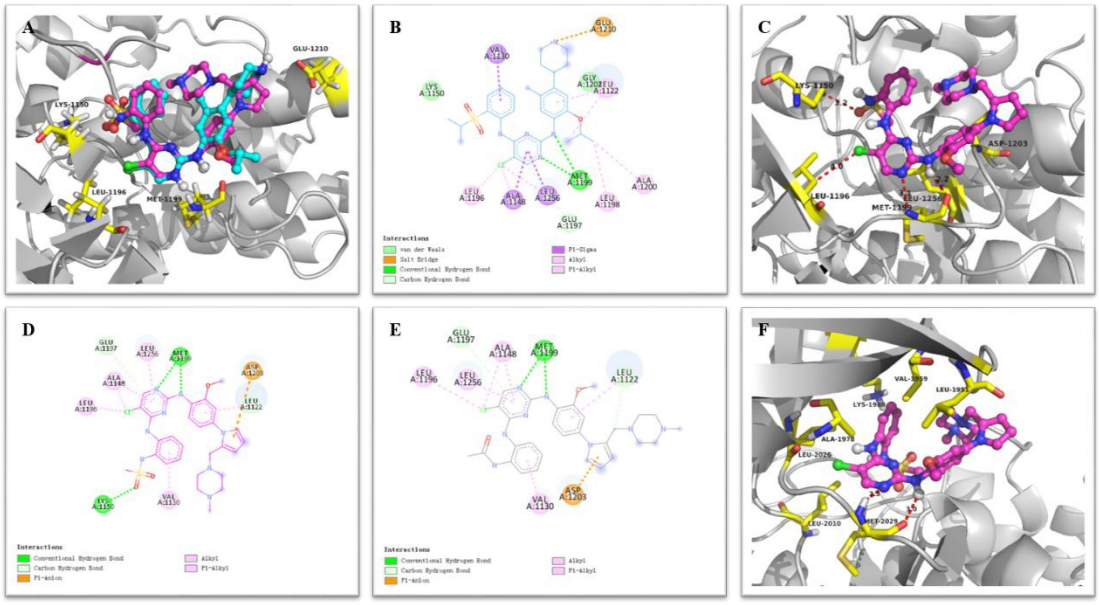

Fig. 4 The binding models of ceritinib, **10d** and **9d** with ALK & ROS1. (A) Predicted binding conformation for **10d** (pink sticks) in the binding site cavity of ALK^{wt} (PDB ID code: 4MKC) and overlapping with ceritinib (blue sticks). (B) 2D diagram of the interaction between ceritinib and ALK. (C) Predicted binding conformation of **10d** in the ATP binding site of ALK. (D) 2D diagram of the interaction between **10d** and ALK. (E) 2D diagram of the interaction between **9d** and ALK. (F) Predicted binding conformation of **10d** in the ATP binding site of ROS1 (PDB ID code: 3ZBF).

4. Conclusion

In this paper, twenty-eight 2,4-diaminopyrimidine compounds (**9a-9n** and **10a-10n**) bearing pyrrolyl moiety were designed and synthesized as ALK and ROS1 dual

inhibitors. Most compounds displayed promising predicted drug-likeness properties and exhibited moderate to excellent activity against Karpas299, H2228 and HCC78, as well as off-target potency toward H460 and A549. The preliminary exploration on a panel of cell lines indicated that compound **10d** bearing sulfonamide (R^1) and 4-methylpiperazinyl (R^2) moiety was of great promising among the compounds with IC_{50} values of 0.01, 0.08 and 0.042 μM against Karpas299, H2228 and HCC78. To our delight, paralleling with cellular results, compound **10d** showed outstanding kinase potency on ALK, ALK^{L1196M} and ROS1 with IC_{50} of 1.8, 4.3 and 3.6 nM, respectively. Moreover, the Hoechst 33258 and AO/EB assay proved clearly that **10d** induced the cell apoptosis in a dose-dependent manner. Finally, molecular dockings exemplified that **10d** could foster potent affinity by forming significant hydrogen and hydrophobic interactions with ALK^{wt} (PDB ID code: 4MKC) and ROS1 (PDB ID code: 3ZBF). In summary, compound **10d** was regarded as a new potential inhibitor and further studies would be discussed and reported in the future.

5. Experimental procedures

5.1. Chemistry

All melting points were obtained on a Büchi Melting Point B-540 apparatus (Büchi Labortechnik, Flawil, Switzerland) and were uncorrected. Mass spectra (MS) were taken in ESI mode on Agilent 1100 LCeMS (Agilent, Palo Alto, CA, USA). The ^1H and ^{13}C NMR were performed using Bruker ARX-400 or ARX-600 spectrometers (Bruker Bioscience, Billerica, MA, USA) with TMS as an internal standard. Column chromatography was run on silica gel (200-300 mesh) from Qingdao Ocean Chemicals (Qingdao, Shandong, China). Unless otherwise noted, all materials were obtained from commercially available sources and were used without further purification.

*5.1.1. Preparation of N^1-(2,5-dichloropyrimidin-4-yl)benzene-1,2-diamine (**3**)*

Benzene-1,2-diamine (17.7 g, 0.16 mol) together with 2,4,5-trichloropyrimidine (30.0 g, 0.16 mol) and DIPEA (54.0 mL, 0.33 mol) was added in isopropanol (300 mL). The reaction mixture was heated and stirred for 2 h at 80 °C. The mixture was filtered immediately. The cake was resuspended in water and adjusted the pH to 7 with hydrochloric acid. The mixture was filtered after stirring for 30 min. The white solid was collected to give **3** in a 96% yield after trituration in dichloromethane and filtration. MS (ESI) m/z: 255.0 $[M+H]^+$.

*5.1.2. General procedure for preparation of compounds (**4a-4b**)*

To a solution of **3** (20.0 g, 0.079 mol) in dichloromethane (100 mL) was added trimethylamine (33.4 mL, 0.24 mol), and the mixture was reacted 2.5 h at room temperature, after which substituted acyl chloride or sulfonyl chloride (7 mL, 0.094 mol) was added dropwise. The reaction mixture was evaporated under reduced pressure whereafter water (200 mL) was poured into the mixture and stirring for 0.5 h. The resulting solids were isolated by filtration and washed with water to give **4a-4b**.

*5.1.2.1. N-(2-((2,5-dichloropyrimidin-4-yl)amino)phenyl)acetamide (**4a**)*

View Article Online
DOI: 10.1039/C9NJ05980F

Yield: 89.0%; MS (ESI) m/z: 297.0 $[M+H]^+$.

*5.1.2.2. N-(2-((2,5-dichloropyrimidin-4-yl)amino)phenyl)methanesulfonamide (**4b**)*
Yield: 85.0%; MS (ESI) m/z: 333.2 $[M+H]^+$.

5.1.3. Preparation of 1-(3-methoxy-4-nitrophenyl)-1H-pyrrole (7)

To a solvent of 4-fluoro-2-methoxy-1-nitrobenzene (20.0 g, 0.12 mol) in *N*,*N*-dimethylformamide (100 mL) was added 1*H*-pyrrole (9 mL, 0.14 mol) and K_2CO_3 (50.0 g, 0.36 mol). The reaction mixture was heated and stirred for 8 h at 100 °C. After cooling to room temperature, the reaction mixture was poured into water (500 mL) and stirred for 1 h. The resulting solid was collected by filtration and washed with water to obtain yellow solid **7** in an 75% yield. MS (ESI) m/z: 219.2 $[M+H]^+$.

*5.1.4. Preparation of 2-methoxy-4-(1H-pyrrol-1-yl)aniline hydrochloride (**8**)*

Iron powder (15.7 g, 0.28 mol) and hydrogen chloride (3.0 mL, 0.2 V/m) was added to ethanol (95%, 200 mL). The resulting solution was heated to 70 °C and stirred for 0.5 h. **7** was added to the suspension. The mixture was stirred for 4 h at 80 °C. After completion of reaction indicated by TLC, the mixture was filtered through diatomite, and the filtrate was removed under reduced pressure. The residue was added water (100 mL) and adjusted pH to 8 with sodium bicarbonate. The solution was extracted with ethyl acetate two times (2×100 mL). The combined organic layers were added 1,4-dioxane of hydrogen chloride and filtered to give the white solid **8** yield 86%. MS (ESI) m/z: 189.1 $[M+H]^+$.

*5.1.5. General procedure for preparation of compounds (**9a** and **10a**)*

A mixture of **4a** or **4b** (0.03 mol) and **8** (9.0 g, 0.04 mol) in isopropanol (100 mL) was refluxed for 24 h. The mixture was filtered immediately when TLC showed the reaction was completed. The cake was resuspended in water and adjusted the pH to 7 with sodium bicarbonate. The mixture was extracted with DCM (2×100 mL). The combined organic layers were evaporated under reduced pressure and purified by column chromatography to gain the solid **9a** and **10a**.

5.1.5.1.
*N-(2-((5-chloro-2-((2-methoxy-4-(1H-pyrrol-1-yl)phenyl)amino)pyrimidin-4-yl)amino)phenyl)acetamide (**9a**)*
Yield: 73.0%; M.p.: 202-205 ºC; MS (ESI) m/z: 449.6 $[M+H]^+$; ^{1}H-NMR (600 MHz, DMSO-d_6) δ_H: 10.03 (s, 1H), 8.55 (s, 1H), 8.14 (s, 1H), 7.90 (d, J = 8.5 Hz, 1H), 7.81 (s, 1H), 7.74 (d, J = 8.0 Hz, 1H), 7.35 (d, J = 7.9 Hz, 1H), 7.33 – 7.28 (m, 3H), 7.24 (dd, J = 11.1, 4.1 Hz, 1H), 7.16 (d, J = 2.4 Hz, 1H), 6.91 (dd, J = 8.6, 2.1 Hz, 1H), 6.25 (t, J = 2.1 Hz, 2H), 3.90 (s, 3H), 2.11 (s, 3H).

5.1.5.2.
*N-(2-((5-chloro-2-((2-methoxy-4-(1H-pyrrol-1-yl)phenyl)amino)pyrimidin-4-yl)amino)phenyl)methanesulfonamide (**10a**)*
Yield: 69.0%; M.p.: 206-207 ºC; MS (ESI) m/z: 485.6 $[M+H]^+$; ^{1}H-NMR (600 MHz, DMSO-d_6) δ_H: 9.29 (s, 1H), 8.56 (s, 1H), 8.16 (s, 1H), 8.00 (s, 1H), 7.94 (d, J = 7.9

Hz, 1H), 7.79 (d, *J* = 8.4 Hz, 1H), 7.40 (dd, *J* = 7.9, 1.3 Hz, 1H), 7.36 – 7.33 (m, 2H), 7.31 (d, *J* = 7.7 Hz, 1H), 7.26 – 7.21 (m, 1H), 7.17 (d, *J* = 2.3 Hz, 1H), 6.94 (dd, *J* = 8.6, 2.0 Hz, 1H), 6.27 – 6.22 (m, 2H), 3.89 (s, 3H), 2.96 (s, 3H) ; ^{13}C-NMR (100 MHz, DMSO- d_6) δ_c: 158.35, 156.36, 155.03, 151.02, 136.25, 134.74, 129.77, 127.50, 127.39, 126.29, 126.03, 125.68, 122.53, 119.73(2C), 111.31, 110.47(2C), 104.90, 103.85, 56.51, 39.52.

*5.1.6. General procedure for preparation of compounds (**9b-9n** and **10b-10n**)*

Various aliphatic amines (0.2 mmol) and formaldehyde (37%, 0.02 g, 0.3 mmol) in acetic acid (5 mL) were stirred 0.5 h at room temperature. Then, **9a** or **10a** which was solved in acetic acid (5 mL) was added slowly to the reaction mixture. After reacting for 1 h, the solvent was evaporated under reduced pressure. The residue was adjusted the pH to 8 with sodium bicarbonate. The mixture was extracted with DCM (2×100 mL). The combined organic layers were evaporated under reduced pressure and purified by column chromatography to gain the solid **9b-9n** and **10b-10n**.

5.1.6.1.
*N-(2-((5-chloro-2-((4-(2-((4-ethylpiperazin-1-yl)methyl)-1H-pyrrol-1-yl)-2-methoxyphenyl)amino)pyrimidin-4-yl)amino)phenyl)acetamide (**9b**)*

Yield: 59.0%; M.p.: 107-109 ºC; MS (ESI) m/z: 573.9 $[M-H]^-$; ^{1}H-NMR (400 MHz, DMSO- d_6) δ_H: 10.02 (s, 1H), 8.59 (s, 1H), 8.16 (s, 1H), 7.96 (d, *J* = 8.6 Hz, 1H), 7.78 (s, 1H), 7.72 (d, *J* = 7.3 Hz, 1H), 7.42 – 7.35 (m, 2H), 7.31 – 7.21 (m, 2H), 6.93 (s, 1H), 6.86 (d, *J* = 8.5 Hz, 1H), 6.13 (d, *J* = 3.2 Hz, 2H), 3.86 (s, 3H), 3.46 – 3.29 (m, 4H), 2.33 (s, 8H), 2.10 (s, 3H), 0.99 (t, *J* = 7.1 Hz, 3H); ^{13}C-NMR (100 MHz, DMSO- d_6) δ_c: 170.09, 157.89, 156.57, 154.96, 148.96, 134.79, 132.11, 131.76, 128.86, 127.52, 127.48, 125.91, 125.64, 124.95, 122.76, 120.05, 116.66, 111.87, 108.58, 108.27, 105.17, 56.50, 53.75, 53.01, 52.91, 52.71, 52.66, 52.04, 23.58, 12.46.

5.1.6.2.
*N-(2-((5-chloro-2-((2-methoxy-4-(2-(morpholinomethyl)-1H-pyrrol-1-yl)phenyl)amino)pyrimidin-4-yl)amino)phenyl)acetamide (**9c**)*

Yield: 67.0%; M.p.: 189-191 ºC; MS (ESI) m/z: 546.8 $[M-H]^-$; ^{1}H-NMR (400 MHz, DMSO- d_6) δ_H: 10.02 (s, 1H), 8.60 (s, 1H), 8.16 (s, 1H), 7.97 (d, *J* = 8.5 Hz, 1H), 7.79 (s, 1H), 7.72 (d, *J* = 7.8 Hz, 1H), 7.39 (s, 1H), 7.37 (s, 1H), 7.28 (dd, *J* = 11.4, 3.9 Hz, 1H), 7.23 (t, *J* = 6.9 Hz, 1H), 6.94 (s, 1H), 6.85 (d, *J* = 8.4 Hz, 1H), 6.14 (d, *J* = 1.7 Hz, 2H), 3.86 (s, 3H), 3.56 (s, 4H), 3.28 (s, 2H), 2.36 (s, 4H), 2.10 (s, 3H); ^{13}C-NMR (100 MHz, DMSO- d_6) δ_c: 170.09, 157.89, 156.59, 154.96, 148.97, 134.74, 132.15, 131.75, 128.38, 127.60, 127.50, 125.90, 125.63, 124.94, 122.92, 120.02, 116.74, 111.99, 108.61, 108.27, 105.18, 66.72 (2C), 56.49, 54.10, 53.27 (2C), 23.58.

5.1.6.3.
*N-(2-((5-chloro-2-((2-methoxy-4-(2-((4-methylpiperazin-1-yl)methyl)-1H-pyrrol-1-yl)phenyl)amino)pyrimidin-4-yl)amino)phenyl)acetamide (**9d**)*

Yield: 49.0%; M.p.: 119-121 ºC; MS (ESI) m/z: 559.4 $[M-H]^-$; ^{1}H-NMR (400 MHz, DMSO- d_6) δ_H: 10.02 (s, 1H), 8.58 (s, 1H), 8.16 (d, *J* = 6.3 Hz, 1H), 7.95 (d, *J* = 8.6 Hz, 1H), 7.78 (s, 1H), 7.72 (d, *J* = 7.8 Hz, 1H), 7.38 (s, 1H), 7.36 (s, 1H), 7.28 (t, *J* =

7.0 Hz, 1H), 7.23 (t, *J* = 7.2 Hz, 1H), 6.93 (s, 1H), 6.85 (d, *J* = 8.6 Hz, 1H), 6.16 – 6.09 (m, 2H), 3.84 (d, *J* = 9.0 Hz, 3H), 3.25 (s, 2H), 2.33 (s, 8H), 2.15 (s, 3H), 2.10 (s, 3H); ^{13}C-NMR (100 MHz, DMSO- d_6) δ_c: 170.93, 158.70, 157.38, 155.77, 149.78, 135.61, 132.91, 132.58, 129.68, 128.32, 128.29, 126.74, 126.46, 125.78, 123.57, 120.87, 117.47, 112.71, 109.37, 109.09, 105.96, 57.31, 56.09 (2C), 54.54, 53.45 (2C), 46.99, 24.37.

5.1.6.4.

*N-(2-((5-chloro-2-((2-methoxy-4-(2-(piperidin-1-ylmethyl)-1H-pyrrol-1-yl)phenyl)amino)pyrimidin-4-yl)amino)phenyl)acetamide (**9e**)*

Yield: 63.0%; M.p.: 108-110 ºC; MS (ESI) m/z: 544.5 $[M-H]^-$; ^{1}H-NMR (400 MHz, DMSO- d_6) δ_H: 10.02 (s, 1H), 8.59 (s, 1H), 8.15 (s, 1H), 7.96 (d, *J* = 8.6 Hz, 1H), 7.78 (s, 1H), 7.71 (d, *J* = 7.9 Hz, 1H), 7.39 (d, *J* = 7.0 Hz, 1H), 7.37 (d, *J* = 7.8 Hz, 1H), 7.27 (dd, *J* = 11.4, 3.8 Hz, 1H), 7.22 (t, *J* = 6.9 Hz, 1H), 6.92 (s, 1H), 6.85 (dd, *J* = 8.6, 1.8 Hz, 1H), 6.14 – 6.08 (m, 2H), 3.86 (s, 3H), 3.22 (s, 2H), 2.33 (s, 4H), 2.09 (s, 3H), 1.47 (s, 4H), 1.39 (s, 2H).

5.1.6.5.

*N-(2-((5-chloro-2-((2-methoxy-4-(2-((4-methylpiperidin-1-yl)methyl)-1H-pyrrol-1-yl)phenyl)amino)pyrimidin-4-yl)amino)phenyl)acetamide (**9f**)*

Yield: 73.0%; M.p.: 111-113 ºC; MS (ESI) m/z: 558.4 $[M-H]^-$; ^{1}H-NMR (400 MHz, DMSO- d_6) δ_H: 10.02 (s, 1H), 8.59 (s, 1H), 8.15 (s, 1H), 7.96 (d, *J* = 8.6 Hz, 1H), 7.78 (s, 1H), 7.72 (d, *J* = 7.0 Hz, 1H), 7.40 – 7.35 (m, 2H), 7.28 (td, *J* = 7.7, 1.4 Hz, 1H), 7.22 (td, *J* = 7.6, 1.3 Hz, 1H), 6.94 – 6.91 (m, 1H), 6.85 (dd, *J* = 8.6, 1.8 Hz, 1H), 6.15 – 6.08 (m, 2H), 3.85 (s, 3H), 3.24 (s, 2H), 2.83 (d, *J* = 10.6 Hz, 2H), 2.10 (s, 3H), 1.90 – 1.81 (m, 2H), 1.58 (d, *J* = 11.3 Hz, 2H), 1.32 (s, 1H), 1.08 – 1.01 (m, 2H), 0.89 (d, J = 6.5 Hz, 3H); ^{13}C-NMR (100 MHz, DMSO- d_6) δ_c: 170.09, 157.90, 156.58, 154.96, 148.98, 134.81, 132.12, 131.78, 128.37, 127.52, 127.47, 125.88, 125.62, 124.96, 122.72, 120.05, 116.73, 111.84, 108.63, 108.27, 105.17, 65.37, 56.41, 54.12, 53.31, 34.46, 30.80, 23.57, 22.24, 15.63.

5.1.6.6.

*N-(2-((5-chloro-2-((2-methoxy-4-(2-(pyrrolidin-1-ylmethyl)-1H-pyrrol-1-yl)phenyl)amino)pyrimidin-4-yl)amino)phenyl)acetamide (**9g**)*

Yield: 67.0%; M.p.: 95-98 ºC; MS (ESI) m/z: 530.4 $[M-H]^-$; ^{1}H-NMR (400 MHz, DMSO- d_6) δ_H: 10.02 (s, 1H), 8.58 (s, 1H), 8.15 (s, 1H), 7.96 (d, *J* = 8.6 Hz, 1H), 7.77 (s, 1H), 7.71 (d, *J* = 7.9 Hz, 1H), 7.46 (s, 1H), 7.37 (d, *J* = 7.8 Hz, 1H), 7.27 (dd, *J* = 10.9, 4.4 Hz, 1H), 7.22 (t, *J* = 7.5 Hz, 1H), 6.93 – 6.89 (m, 1H), 6.86 (dd, *J* = 8.6, 1.9 Hz, 1H), 6.15 – 6.10 (m, 2H), 3.83 (s, 3H), 3.41 (s, 2H), 2.45 (s, 4H), 2.09 (s, 3H), 1.70 (s, 4H); ^{13}C-NMR (100 MHz, DMSO- d_6) δ_c: 170.08, 157.88, 156.59, 154.96, 148.97, 134.75, 132.15, 131.75, 130.43, 127.56, 127.42, 125.89, 125.61, 124.93, 122.31, 120.05, 116.44, 110.77, 108.51, 108.33, 105.12, 56.21, 53.65 (2C), 51.10, 23.57, 23.52 (2C).

View Article Online
DOI: 10.1039/C9NJ05980F

5.1.6.7.

*N-(2-((5-chloro-2-((2-methoxy-4-(2-(thiomorpholinomethyl)-1H-pyrrol-1-yl)phenyl)amino)pyrimidin-4-yl)amino)phenyl)acetamide (**9h**)*

Yield: 59.0%; M.p.: 96-98 ºC; MS (ESI) m/z: 562.4 $[M-H]^-$; ^{1}H-NMR (400 MHz, DMSO- d_6) δ_H: 10.01 (s, 1H), 8.59 (s, 1H), 8.15 (s, 1H), 7.96 (d, J = 8.6 Hz, 1H), 7.79 (s, 1H), 7.71 (d, J = 7.7 Hz, 1H), 7.39 – 7.35 (m, 1H), 7.28 (dd, J = 11.4, 3.8 Hz, 1H), 7.26 – 7.21 (m, 2H), 6.94 – 6.89 (m, 1H), 6.85 (dd, J = 8.6, 2.0 Hz, 1H), 6.14 – 6.10 (m, 2H), 3.86 (s, 3H), 3.30 (s, 2H), 2.57 (s, 4H), 2.55 (s, 4H), 2.09 (s, 3H); ^{13}C-NMR (100 MHz, DMSO- d_6) δ_c: 170.09, 157.89, 156.59, 154.97, 148.97, 134.78, 132.15, 131.75, 128.70, 127.66, 127.51, 125.88, 125.64, 124.93, 123.03, 119.95, 117.07, 111.90, 108.71, 108.20, 105.16, 56.56, 54.48 (2C), 54.39, 27.77 (2C), 23.57.

5.1.6.8.

*N-(2-((5-chloro-2-((4-(2-((1,1-dioxidothiomorpholino)methyl)-1H-pyrrol-1-yl)-2-methoxyphenyl)amino)pyrimidin-4-yl)amino)phenyl)acetamide (**9i**)*

Yield: 61.0%; M.p.: 144-147 ºC; MS (ESI) m/z: 594.5 $[M-H]^-$; ^{1}H-NMR (400 MHz, DMSO- d_6) δ_H: 9.99 (s, 1H), 8.60 (s, 1H), 8.16 (s, 1H), 7.97 (d, J = 8.5 Hz, 1H), 7.83 (s, 1H), 7.70 (d, J = 7.3 Hz, 1H), 7.38 (d, J = 7.7 Hz, 1H), 7.29 (t, J = 6.8 Hz, 1H), 7.26 – 7.21 (m, 1H), 6.97 (d, J = 1.9 Hz, 1H), 6.74 (d, J = 8.4 Hz, 1H), 6.08 (s, 2H), 3.83 (s, 3H), 3.35 (s, 2H), 2.94 (s, 4H), 2.69 (s, 4H), 2.09 (s, 3H).

5.1.6.9.

*N-(2-((5-chloro-2-((4-(2-(((2-hydroxyethyl)amino)methyl)-1H-pyrrol-1-yl)-2-methoxyphenyl)amino)pyrimidin-4-yl)amino)phenyl)acetamide (**9j**)*

Yield: 71.0%; M.p.: 94-96 ºC; MS (ESI) m/z: 520.7 $[M-H]^-$; ^{1}H-NMR (400 MHz, DMSO- d_6) δ_H: 10.02 (s, 1H), 8.58 (s, 1H), 8.15 (s, 1H), 7.95 (d, J = 8.5 Hz, 1H), 7.79 (s, 1H), 7.71 (d, J = 7.8 Hz, 1H), 7.36 (d, J = 7.8 Hz, 1H), 7.33 (d, J = 2.1 Hz, 1H), 7.28 (dd, J = 11.4, 3.9 Hz, 1H), 7.23 (t, J = 6.9 Hz, 1H), 6.90 – 6.87 (m, 1H), 6.83 (dd, J = 8.6, 2.0 Hz, 1H), 6.15 (d, J = 1.5 Hz, 1H), 6.12 (t, J = 3.1 Hz, 1H), 4.51 (s, 1H), 3.85 (s, 3H), 3.60 (s, 2H), 3.45 (d, J = 4.6 Hz, 2H), 2.59 (t, J = 5.6 Hz, 2H), 2.09 (s, 3H).

5.1.6.10.

*N-(2-((5-chloro-2-((4-(2-((diethylamino)methyl)-1H-pyrrol-1-yl)-2-methoxyphenyl)amino)pyrimidin-4-yl)amino)phenyl)acetamide (**9k**)*

Yield: 53.0%; M.p.: 79-81 ºC; MS (ESI) m/z: 532.6 $[M-H]^-$; ^{1}H-NMR (400 MHz, DMSO- d_6) δ_H: 10.02 (s, 1H), 8.59 (s, 1H), 8.15 (s, 1H), 7.96 (d, J = 8.6 Hz, 1H), 7.78 (s, 1H), 7.71 (d, J = 7.8 Hz, 1H), 7.40 – 7.33 (m, 1H), 7.31 – 7.18 (m, 3H), 6.90 – 6.83 (m, 2H), 6.16 – 6.08 (m, 2H), 3.84 (s, 3H), 3.39 (s, 2H), 2.45 (d, J = 6.4 Hz, 4H), 2.09 (s, 3H), 0.85 (t, J = 7.1 Hz, 6H).

5.1.6.11.

*N-(2-((5-chloro-2-((4-(2-((4-(2-hydroxyethyl)piperazin-1-yl)methyl)-1H-pyrrol-1-yl)-2-methoxyphenyl)amino)pyrimidin-4-yl)amino)phenyl)acetamide (**9l**)*

Yield: 63.0%; M.p.: 191-194 ºC; MS (ESI) m/z: 589.8 $[M-H]^-$; ^{1}H-NMR (400 MHz, DMSO- d_6) δ_H: 10.02 (s, 1H), 8.58 (s, 1H), 8.15 (s, 1H), 7.95 (d, J = 8.6 Hz, 1H), 7.78

(s, 1H), 7.71 (d, *J* = 7.8 Hz, 1H), 7.39 – 7.34 (m, 2H), 7.28 (dd, *J* = 11.4, 3.8 Hz, 1H), 7.23 (dd, *J* = 11.3, 3.8 Hz, 1H), 6.95 – 6.90 (m, 1H), 6.85 (dd, *J* = 8.6, 1.9 Hz, 1H), 6.16 – 6.07 (m, 2H), 4.38 (s, 1H), 3.86 (s, 3H), 3.48 (dd, *J* = 11.0, 5.8 Hz, 2H), 3.25 (s, 2H), 2.46 – 2.29 (m, 10H), 2.09 (s, 3H).

5.1.6.12.
*N-(2-((5-chloro-2-((4-(2-((dimethylamino)methyl)-1H-pyrrol-1-yl)-2-methoxyphenyl) amino)pyrimidin-4-yl)amino)phenyl)acetamide (**9m**)*
Yield: 43.0%; M.p.: 206-207 ºC; MS (ESI) m/z: 504.7 $[M-H]^-$; ^{1}H-NMR (400 MHz, DMSO- d_6) δ_H: 10.02 (s, 1H), 8.58 (s, 1H), 8.15 (s, 1H), 7.96 (d, *J* = 8.6 Hz, 1H), 7.78 (s, 1H), 7.71 (d, *J* = 6.8 Hz, 1H), 7.40 – 7.34 (m, 2H), 7.28 (td, *J* = 7.6, 1.4 Hz, 1H), 7.23 (td, *J* = 7.6, 1.4 Hz, 1H), 6.93 (t, *J* = 2.3 Hz, 1H), 6.87 (dd, *J* = 8.6, 2.0 Hz, 1H), 6.15 – 6.10 (m, 2H), 3.85 (s, 3H), 3.22 (s, 2H), 2.15 (s, 6H), 2.09 (s, 3H).

5.1.6.13.
*N-(2-((5-chloro-2-((4-(2-((3-hydroxyazetidin-1-yl)methyl)-1H-pyrrol-1-yl)-2-methoxy phenyl)amino)pyrimidin-4-yl)amino)phenyl)acetamide (**9n**)*
Yield: 64.0%; M.p.: 114-117 ºC; MS (ESI) m/z: 532.6 $[M-H]^-$; ^{1}H-NMR (400 MHz, DMSO- d_6) δ_H: 10.03 (s, 1H), 8.58 (s, 1H), 8.15 (s, 1H), 7.94 (d, *J* = 8.5 Hz, 1H), 7.79 (s, 1H), 7.71 (d, *J* = 7.6 Hz, 1H), 7.37 (d, *J* = 7.7 Hz, 1H), 7.34 (d, *J* = 1.8 Hz, 1H), 7.31 – 7.27 (m, 1H), 7.26 – 7.21 (m, 1H), 6.91 – 6.89 (m, 1H), 6.85 (dd, *J* = 8.6, 1.7 Hz, 1H), 6.13 – 6.08 (m, 2H), 5.28 (d, *J* = 6.3 Hz, 1H), 4.19 (dd, *J* = 12.0, 6.0 Hz, 1H), 3.85 (s, 3H), 3.46 (t, *J* = 6.6 Hz, 2H), 3.40 (s, 2H), 2.75 (t, *J* = 6.5 Hz, 2H), 2.10 (s, 3H).

5.1.6.14.
*N-(2-((5-chloro-2-((4-(2-((4-ethylpiperazin-1-yl)methyl)-1H-pyrrol-1-yl)-2-methoxyp henyl)amino)pyrimidin-4-yl)amino)phenyl)methanesulfonamide (**10b**)*
Yield: 45.0%; M.p.: 196-198 ºC; MS (ESI) m/z: 609.5 $[M-H]^-$; ^{1}H-NMR (400 MHz, DMSO- d_6) δ_H: 9.30 (s, 1H), 8.66 (s, 1H), 8.18 (s, 1H), 7.95 (s, 1H), 7.92 (d, *J* = 7.8 Hz, 1H), 7.87 (d, *J* = 8.6 Hz, 1H), 7.43 – 7.37 (m, 2H), 7.26 (dd, *J* = 11.5, 3.9 Hz, 1H), 7.24 – 7.19 (m, 1H), 6.97 – 6.93 (m, 1H), 6.89 (dd, *J* = 8.6, 1.9 Hz, 1H), 6.15 – 6.10 (m, 2H), 3.85 (s, 3H), 3.28 (s, 2H), 2.93 (s, 3H), 2.37 – 2.32 (m, 10H), 0.99 (t, *J* = 7.1 Hz, 3H); ^{13}C-NMR (100 MHz, DMSO- d_6) δ_c: 158.12, 156.47, 155.02, 149.66, 135.24, 134.26, 130.78, 128.79, 127.41, 126.74 (2C), 126.11, 125.78, 122.81, 121.01, 116.60, 111.99, 108.65, 108.32, 105.16, 108.20, 105.16, 65.38, 56.47, 55.14 (2C), 53.68, 52.43 (2C), 45.94.
3.1.6.15.

5.1.6.15.
*N-(2-((5-chloro-2-((2-methoxy-4-(2-(morpholinomethyl)-1H-pyrrol-1-yl)phenyl)amin o)pyrimidin-4-yl)amino)phenyl)methanesulfonamide (**10c**)*
Yield: 73.0%; M.p.: 199-202 ºC; MS (ESI) m/z: 582.4 $[M-H]^-$; ^{1}H-NMR (400 MHz, DMSO- d_6) δ_H: 9.30 (s, 1H), 8.62 (s, 1H), 8.19 (s, 1H), 7.95 (s, 1H), 7.92 – 7.84 (m, 2H), 7.44 – 7.39 (m, 2H), 7.31 (t, *J* = 7.0 Hz, 1H), 7.24 (t, *J* = 6.9 Hz, 1H), 6.95 (t, *J* = 2.2 Hz, 1H), 6.88 (dd, *J* = 8.6, 1.8 Hz, 1H), 6.16 – 6.11 (m, 2H), 3.85 (s, 3H), 3.55 (s,

4H), 3.29 (s, 2H), 2.95 (s, 3H), 2.36 (s, 4H); ^{13}C-NMR (100 MHz, DMSO- d_6) δ_c: 158.08, 156.57, 155.08, 149.61, 135.18, 134.42, 130.36, 128.33, 127.44, 127.25, 127.14, 126.55, 125.93, 122.93, 120.91, 116.64, 112.08, 108.67, 108.31, 105.14, 66.71(2C), 56.44(2C), 54.11 , 53.27(2C).

5.1.6.16.
*N-(2-((5-chloro-2-((2-methoxy-4-(2-((4-methylpiperazin-1-yl)methyl)-1H-pyrrol-1-yl) phenyl)amino)pyrimidin-4-yl)amino)phenyl)methanesulfonamide (**10d**)*
Yield: 53.0%; M.p.: 191-193 ºC; MS (ESI) m/z: 595.4 $[M-H]^-$; ^{1}H-NMR (400 MHz, DMSO- d_6) δ_H: 9.32 (s, 1H), 8.65 (s, 1H), 8.18 (s, 1H), 7.95 (s, 1H), 7.92 (d, J = 7.7 Hz, 1H), 7.87 (d, J = 8.6 Hz, 1H), 7.43 – 7.37 (m, 2H), 7.27 (dd, J = 12.3, 5.8 Hz, 1H), 7.22 (t, J = 6.9 Hz, 1H), 6.95 (d, J = 1.9 Hz, 1H), 6.92 – 6.84 (m, 1H), 6.17 – 6.13 (m, 2H), 3.85 (s, 3H), 3.27 (s, 2H), 2.93 (s, 3H), 2.36 (s, 8H), 2.18 (s, 3H).

5.1.6.17.
*N-(2-((5-chloro-2-((2-methoxy-4-(2-(piperidin-1-ylmethyl)-1H-pyrrol-1-yl)phenyl)ami no)pyrimidin-4-yl)amino)phenyl)methanesulfonamide (**10e**)*
Yield: 51.0%; M.p.: 178-181 ºC; MS (ESI) m/z: 580.4 $[M-H]^-$; ^{1}H-NMR (400 MHz, DMSO- d_6) δ_H: 9.29 (s, 1H), 8.62 (s, 1H), 8.18 (s, 1H), 7.95 (s, 1H), 7.91 (d, J = 7.9 Hz, 1H), 7.87 (d, J = 8.6 Hz, 1H), 7.44 – 7.37 (m, 2H), 7.29 (dd, J = 11.5, 3.9 Hz, 1H), 7.25 – 7.20 (m, 1H), 6.96 – 6.92 (m, 1H), 6.88 (dd, J = 8.6, 2.0 Hz, 1H), 6.16 – 6.09 (m, 2H), 3.85 (s, 3H), 3.26 (s, 2H), 2.94 (s, 3H), 2.34 (s, 4H), 1.46 (d, J = 4.6 Hz, 4H), 1.39 (s, 2H); ^{13}C-NMR (100 MHz, DMSO- d_6) δ_c: 158.10, 156.51, 155.05, 149.62, 135.24, 134.38, 130.49, 128.90, 127.41, 127.05, 126.99, 126.33, 125.83, 122.78, 120.95, 116.69, 111.99, 108.73, 108.31, 105.15, 65.38, 56.39, 54.39, 53.87(2C), 25.94 (2C), 24.41.

5.1.6.18.
*N-(2-((5-chloro-2-((2-methoxy-4-(2-((4-methylpiperidin-1-yl)methyl)-1H-pyrrol-1-yl) phenyl)amino)pyrimidin-4-yl)amino)phenyl)methanesulfonamide (**10f**)*
Yield: 67.0%; M.p.: 106-108 ºC; MS (ESI) m/z: 596.8 $[M+H]^+$; ^{1}H-NMR (400 MHz, DMSO- d_6) δ_H: 9.29 (s, 1H), 8.62 (s, 1H), 8.18 (s, 1H), 7.96 (s, 1H), 7.91 (d, J = 7.9 Hz, 1H), 7.87 (d, J = 8.5 Hz, 1H), 7.44 – 7.38 (m, 2H), 7.29 (t, J = 7.0 Hz, 1H), 7.23 (t, J = 6.9 Hz, 1H), 6.94 (d, J = 2.1 Hz, 1H), 6.88 (dd, J = 8.6, 1.9 Hz, 1H), 6.16 – 6.09 (m, 2H), 3.85 (s, 3H), 3.27 (s, 2H), 2.94 (s, 3H), 2.84 (d, J = 11.3 Hz, 2H), 1.88 (t, J = 12.0 Hz, 2H), 1.58 (d, J = 11.8 Hz, 2H), 1.32 (s, 1H), 1.09 – 1.00 (m, 2H), 0.88 (d, J = 6.5 Hz, 3H).

5.1.6.19.
*N-(2-((5-chloro-2-((2-methoxy-4-(2-(pyrrolidin-1-ylmethyl)-1H-pyrrol-1-yl)phenyl)a mino)pyrimidin-4-yl)amino)phenyl)methanesulfonamide (**10g**)*
Yield: 37.0%; M.p.: 97-99 ºC; MS (ESI) m/z: 566.4 $[M-H]^-$; ^{1}H-NMR (400 MHz, DMSO- d_6) δ_H: 9.38 (s, 1H), 8.65 (s, 1H), 8.18 (s, 1H), 7.95 (s, 1H), 7.90 (d, J = 7.8 Hz, 1H), 7.87 (d, J = 8.6 Hz, 1H), 7.48 (d, J = 2.0 Hz, 1H), 7.41 (dd, J = 7.7, 1.4 Hz, 1H), 7.28 (td, J = 7.7, 1.4 Hz, 1H), 7.22 (td, J = 7.6, 1.4 Hz, 1H), 6.95 – 6.92 (m, 1H),

6.88 (dd, J = 8.6, 2.0 Hz, 1H), 6.19 – 6.09 (m, 2H), 3.83 (s, 3H), 3.46 (s, 2H), 2.94 (s, 3H), 2.48 (s, 4H), 1.70 (s, 4H).

5.1.6.20.
*N-(2-((5-chloro-2-((2-methoxy-4-(2-(thiomorpholinomethyl)-1H-pyrrol-1-yl)phenyl)amino)pyrimidin-4-yl)amino)phenyl)methanesulfonamide (**10h**)*
Yield: 42.0%; M.p.: 106-109 ºC; MS (ESI) m/z: 598.4 $[M-H]^-$; ^{1}H-NMR (400 MHz, DMSO- d_6) δ_H: 9.30 (s, 1H), 8.62 (s, 1H), 8.19 (s, 1H), 7.96 (s, 1H), 7.90 (d, J = 8.4 Hz, 1H), 7.87 (d, J = 8.6 Hz, 1H), 7.41 (dd, J = 7.8, 1.3 Hz, 1H), 7.31 (t, J = 7.0 Hz, 1H), 7.28 – 7.21 (m, 2H), 6.95 – 6.92 (m, 1H), 6.87 (dd, J = 8.6, 1.9 Hz, 1H), 6.15 – 6.09 (m, 2H), 3.86 (s, 3H), 2.95 (s, 3H), 2.58 (d, J = 5.4 Hz, 4H), 2.55 (s, 4H).

5.1.6.21.
*N-(2-((5-chloro-2-((4-(2-((1,1-dioxidothiomorpholino)methyl)-1H-pyrrol-1-yl)-2-methoxyphenyl)amino)pyrimidin-4-yl)amino)phenyl)methanesulfonamide (**10i**)*
Yield: 79.0%; M.p.: 116-119 ºC; MS (ESI) m/z: 654.8 $[M+Na]^+$; ^{1}H-NMR (400 MHz, DMSO- d_6) δ_H: 9.30 (s, 1H), 8.62 (s, 1H), 8.18 (s, 1H), 7.97 (s, 1H), 7.92 – 7.84 (m, 2H), 7.41 (dd, J = 7.8, 1.3 Hz, 1H), 7.32 (t, J = 7.0 Hz, 1H), 7.26 (dd, J = 10.8, 4.4 Hz, 1H), 7.20 (d, J = 2.1 Hz, 1H), 6.97 – 6.93 (m, 1H), 6.87 (dd, J = 8.6, 1.9 Hz, 1H), 6.18 (d, J = 1.6 Hz, 1H), 6.15 (t, J = 3.1 Hz, 1H), 3.86 (s, 3H), 3.51 (s, 2H), 3.02 (s, 4H), 2.95 (s, 3H), 2.83 (s, 4H).

5.1.6.22.
*N-(2-((5-chloro-2-((4-(2-(((2-hydroxyethyl)amino)methyl)-1H-pyrrol-1-yl)-2-methoxyphenyl)amino)pyrimidin-4-yl)amino)phenyl)methanesulfonamide (**10j**)*
Yield: 64.0%; M.p.: 159-162 ºC; MS (ESI) m/z: 556.7 $[M-H]^-$; ^{1}H-NMR (400 MHz, DMSO- d_6) δ_H: 8.65 (s, 1H), 8.18 (s, 1H), 7.96 (s, 1H), 7.92 – 7.85 (m, 2H), 7.43 – 7.38 (m, 2H), 7.30 – 7.25 (m, 1H), 7.23 (t, J = 7.4 Hz, 1H), 6.96 (s, 1H), 6.93 – 6.89 (m, 1H), 6.18 (d, J = 1.6 Hz, 1H), 6.15 (t, J = 3.1 Hz, 1H), 4.21 (s, 2H), 3.84 (s, 3H), 3.65 (t, J = 6.8 Hz, 2H), 3.51 (s, 2H), 2.97 – 2.91 (m, 5H); ^{13}C-NMR (100 MHz, DMSO- d_6) δ_c: 158.09, 156.55, 155.02, 149.67, 135.08, 134.24, 130.80, 130.24, 127.51, 126.85, 126.84, 126.74, 126.33, 125.86, 122.94, 120.98, 116.64, 111.25, 108.72, 108.41, 105.16, 65.38, 62.83, 56.38, 51.74, 48.84.

5.1.6.23.
*N-(2-((5-chloro-2-((4-(2-((diethylamino)methyl)-1H-pyrrol-1-yl)-2-methoxyphenyl)amino)pyrimidin-4-yl)amino)phenyl)methanesulfonamide (**10k**)*
Yield: 81%; M.p.: 138-141 ºC; MS (ESI) m/z: 568.3 $[M-H]^-$; ^{1}H-NMR (400 MHz, DMSO- d_6) δ_H: 9.31 (s, 1H), 8.63 (s, 1H), 8.18 (s, 1H), 7.95 (s, 1H), 7.91 – 7.86 (m, 2H), 7.44 – 7.38 (m, 1H), 7.32 – 7.19 (m, 3H), 6.91 – 6.86 (m, 2H), 6.15 – 6.12 (m, 2H), 3.84 (s, 3H), 3.45 (s, 2H), 2.94 (s, 3H), 2.50 – 2.43 (m, 4H), 0.85 (t, J = 7.1 Hz, 6H).

5.1.6.24.
*N-(2-((5-chloro-2-((4-(2-((4-(hydroxymethyl)piperazin-1-yl)methyl)-1H-pyrrol-1-yl)-2-methoxyphenyl)amino)pyrimidin-4-yl)amino)phenyl)methanesulfonamide (**10l**)*

View Article Online
DOI: 10.1039/C9NJ05980F

Yield: 48%; M.p.: 109-112 ºC; MS (ESI) m/z: 625.8 [M-H]$^-$; ^{1}H-NMR (400 MHz, DMSO- d_6) δ_H: 9.30 (s, 1H), 8.64 (s, 1H), 8.18 (s, 1H), 7.95 (s, 1H), 7.91 (d, J = 7.8 Hz, 1H), 7.87 (d, J = 8.5 Hz, 1H), 7.43 – 7.38 (m, 2H), 7.31 – 7.25 (m, 1H), 7.23 (dd, J = 12.0, 4.5 Hz, 1H), 6.96 – 6.93 (m, 1H), 6.89 (dd, J = 8.6, 1.9 Hz, 1H), 6.15 – 6.10 (m, 2H), 4.40 (s, 1H), 3.85 (s, 3H), 3.49 (s, 2H), 3.27 (s, 2H), 2.94 (s, 3H), 2.46 – 2.35 (m, 10H); ^{13}C-NMR (100 MHz, DMSO- d_6) δ_c: 158.11, 156.49, 155.03, 149.64, 135.23, 134.30, 130.68, 128.80, 127.41, 126.84, 126.21, 125.82, 122,80, 120.97, 116.61, 111.95, 108.67, 108.32, 105.16, 65.38, 65.56, 58.77, 56.48(2C), 53.73, 53.66 (2C), 52.55.

5.1.6.25.
*N-(2-((5-chloro-2-((4-(2-((dimethylamino)methyl)-1H-pyrrol-1-yl)-2-methoxyphenyl) amino)pyrimidin-4-yl)amino)phenyl)methanesulfonamide (**10m**)*
Yield: 58%; M.p.: 165-168 ºC; MS (ESI) m/z: 540.8 [M-H]$^-$; ^{1}H-NMR (400 MHz, DMSO- d_6) δ_H: 9.14 (s, 1H), 8.16 – 8.08 (m, 2H), 8.02 – 7.94 (m, 2H), 7.44 (d, J = 2.1 Hz, 1H), 7.26 (dd, J = 7.9, 1.1 Hz, 1H), 7.03 – 6.91 (m, 3H), 6.82 (t, J = 7.2 Hz, 1H), 6.17 – 6.09 (m, 2H), 3.86 (s, 3H), 3.24 (s, 2H), 2.15 (s, 6H), 1.89 (s, 3H).

5.1.6.26.
*N-(2-((5-chloro-2-((4-(2-((3-hydroxyazetidin-1-yl)methyl)-1H-pyrrol-1-yl)-2-methoxy phenyl)amino)pyrimidin-4-yl)amino)phenyl)methanesulfonamide (**10n**)*
Yield: 53%; M.p.: 232-235 ºC; MS (ESI) m/z: 568.6 [M-H]$^-$; ^{1}H-NMR (400 MHz, DMSO- d_6) δ_H: 9.33 (s, 1H), 8.63 (s, 1H), 8.18 (s, 1H), 7.97 (s, 1H), 7.90 (d, J = 7.5 Hz, 1H), 7.85 (d, J = 8.5 Hz, 1H), 7.41 (d, J = 7.7 Hz, 1H), 7.35 (d, J = 1.8 Hz, 1H), 7.30 (t, J = 7.1 Hz, 1H), 7.24 (t, J = 7.0 Hz, 1H), 6.92 (s, 1H), 6.88 (dd, J = 8.6, 1.7 Hz, 1H), 6.16 – 6.09 (m, 2H), 5.30 (d, J = 6.3 Hz, 1H), 4.22 – 4.14 (m, 1H), 3.85 (s, 3H), 3.52 – 3.43 (m, 4H), 2.94 (s, 3H), 2.79 (t, J = 6.7 Hz, 2H).

5.2. Physical properties and MTT assay in vitro

Physical properties such as Log P and topological polar surface area (TPSA) were calculated for each compounds using Discovery Studio 2017 and SwissADME (http://swissadme.ch/index.php#).

The cytotoxic activities of compounds **9a-9n** and **10a-10n** were evaluated against Karpas299, H2228, HCC78, A549 and H460 by the standard MTT assay *in vitro*, with ceritinib as the positive control. The cancer cell lines were cultured in minimum essential medium (MEM) supplement with 10% fetal bovine serum (FBS). Approximate 4×103 cells, suspended in MEM medium, were plated into each well of a 96-well plate and incubated in 5% CO_2 at 37 °C for 24 h. The tested compounds at the indicated final concentrations were added to the culture medium and incubated for 72 h. Fresh MTT was added to each well at the terminal concentration of 5 μM, and incubated with cells at 37 °C for 4 h. The formazan crystals in each well were dissolved in 100 μL DMSO, and the absorbency at 492 nm (for absorbance of MTT formazan) and 630 nm (for the reference wavelength) was measured with an ELISA reader. All of the compounds were tested three times in each of the cell lines. The results, expressed as IC_{50} (inhibitory concentration 50%),

were the averages of three determinations and calculated relative to the vehicle (DMSO) control by the Bacus Laboratories Incorporated Slide Scanner (Bliss) software.

5.3. In vitro enzymatic assays

The *in vitro* enzymatic assays versus ALK, ALK^{L1196M}, ROS1 and EGFR were evaluated by homogeneous time-resolved fluorescence (HTRF) assay. In enzymatic assay, the solution of peptide substrates, ATP, appropriate kinase, and diluted compound was mixed with the kinase reaction buffer (50 mM HEPES, pH 7.5, 0.0015% Brij-35, 10 mM $MgCl_2$, 2 mM DTT), with blank DMSO solution as the negative control. The kinase reaction was initiated by the addition of tyrosine kinase proteins diluted in 39 μL of kinase reaction buffer solution and incubated at 28 °C for 1 h. And then add 25 μL of stop buffer (100 mM HEPES, pH 7.5, 0.015% Brij-35, 0.2% Coating Reagent #3, 50 mM EDTA) to stop reaction. The plate was read by Caliper at 320 nm and 615 nm. IC_{50} values were calculated from the inhibition curves.

5.4. Morphology analysis of apoptotic cells and nuclear morphology assays

Apoptotic morphological changes of Karpas299 cells was detected by AO/EB staining. Briefly, cells were seeded in six-well plates for 24 h, and then treated with ceritinib (25 nM) or different concentrations (25 nM and 50 nM) of **10d** for 48 h. The cells were washed with phosphate buffer saline (PBS) and then stained with AO/EB mixed solution (AO: EB ¼ 1:1) for a quarter. The stained cells were washed twice with PBS and observed by fluorescence microscope.

To investigate the apoptotic morphological changes of nuclear chromatin in Karpas299 cells, Hoechst 33258 staining was performed. In brief, cells were seeded in six-well plates overnight, and then treated with ceritinib (50 nM) or different concentrations (25 nM and 50 nM) of **10d**. After 48 h, the medium was discarded and the cells were washed with PBS. After that, the cells were stained with Hoechst 33258 solution for 15 min. The stained cells were washed twice with PBS and observed by fluorescence microscope.

5.5. Molecular docking

The molecular docking was performed with Accelrys Discovery Studio 2017. The protein files (PDB ID code: 4MKC and 3ZBF) were obtained from Protein Data Bank (http://www.rcsb.org/pdb/). During the docking process, the protein was prepared through several steps, such as standardization of atom names and insertion of missing atoms in residues. Then, the protein model was typed with the CHARMm force field and a binding sphere within 50 Å radius was defined as the binding site around the reference ligand (ceritinib). Ceritinib, and were drawn with ChemBioDraw 3D and fully minimized using the CHARMm force field. Finally, they were searching for possible conformations in the binding site using the CDOCKER protocol with default settings. The binding results were viewed using Discovery Studio 2017 and the 2D binding mode figures were generated from it. All 3D figures were generated from Pymol (The Pymol Molecular Graphics System, Version 1.4.1. Schrodinger, LLC).

View Article Online
DOI: 10.1039/C9NJ05980F

Conflict of interest

The authors have declared no conflict of interest.

Acknowledgements

This work was supported by National Natural Science Foundation of China (No.81673308), Youth Backbone Talent Training Project of Shenyang Pharmaceutical University (No. ZQN2018008) and Development Project of Ministry of Education Innovation Team (No. IRT1073).

References

1 K. Pulford, L. Lamant, S.W. Morris, L.H. Butler, K.M. Wood, D. Stroud, G. Delsol and D.Y. Mason, *Blood.*, 1997, **89**(4), 1394-1404.
2 K. Rikova, A. Guo, Q. Zeng, A. Possemato, J. Yu, H. Haack, J. Nardone, K. Lee, C. Reeves, Y. Li, Y. Hu, Z. Tan, M. Stokes, L. Sullivan, J. Mitchell, R. Wetzel, J. Macneill, J.M. Ren, J. Yuan, C.E. Bakalarski, J. Villen, J.M. Kornhauser, B. Smith, D. Li, X. Zhou, S.P. Gygi, T. Gu, R.D. Polakiewicz, J. Rush and M.J. Comb, *Cell.*, 2007, **131**(6), 1190-1203.
3 B. Golding, A. Luu, R. Jones and A.M. Viloria-Petit, *Mol. Cancer.,* 2018, **17**(1), 52-66.
4 M. Soda, Y.L. Choi, M. Enomoto, S. Takada, Y. Yamashita, S. Ishikawa, S. Fujiwara, H. Watanabe, K. Kurashina, H. Hatanaka, M. Bando, S. Ohno, Y. Ishikawa, H. Aburatani, T. Niki, Y. Sohara, Y. Sugiyama and H. Mano, *Nature.*, 2007, **448**(7153), 561-566.
5 H.Y. Zou, Q. Li, J.H. Lee, M.E. Arango, S.R. McDonnell, S. Yamazaki, T.B. Koudriakova, G. Alton, J.J. Cui, P.P. Kung, M.D. Nambu, G. Los, S.L. Bender, B. Mroczkowski and J.G. Christensen, *Cancer. Res.*, 2007, **67**(9), 4408-4417.
6 K.D. Davies, A.T. Le, M.F. Theodoro, M.C. Skokan, D.L. Aisner, E.M. Berge, L.M. Terracciano, F. Cappuzzo, M. Incarbone, M. Roncalli, M. Alloisio, A. Santoro, D.R. Camidge, M. Varella-Garcia and R.C. Doebele, *Clin. Cancer. Res.*, 2012, **18**(17), 4570-4579.
7 S.H. Ou, J. Tan, Y. Yen and R.A. Soo, *Expert. Rev. Anticancer. Ther.*, 2012, **12**(4), 447-456.
8 Y. Wang, S. Chen, G. Hu, J. Wang, W.F. Gou, D.Y. Zuo, Y.C. Gu, P. Gong and X. Zhai, *Eur. J. Med. Chem.*, 2018, **143**, 123-136.
9 J.G. Christensen, H.Y. Zou, M.E. Arango, Q. Li, J.H. Lee, S.R. McDonnell, S. Yamazaki, G.R. Alton, B. Mroczkowski and G. Los, *Mol. Cancer. Ther.*, 2007, **6**(12), 3314-3322.
10 A.T. Shaw, B.Y. Yeap, B.J. Solomon, G.J. Riely, J. Gainor, J.A. Engelman, G.I. Shapiro, D.B. Costa, S.I. Ou, M. Butaney, R. Salgia, R.G. Maki, M. Varella-Garcia, R.C. Doebele, Y. Bang, K. Kulig, P. Selaru, Y. Tang, K.D. Wilner, E.L. Kwak, J.W. Clark, A.J. Iafrate and D.R. Camidge, *Lancet Oncol.*, 2011, **12**(11), 1004-1012.

11 R.C. Doebele, A.B. Pilling, D.L. Aisner, T.G. Kutateladze, A.T. Le, A.J. Weickhardt, K.L. Kondo, D.J. Linderman, L.E. Heasley, W.A. Franklin, M. Varella-Garcia and D.R. Camidge, *Clin. Cancer. Res.*, 2012, **18**(5), 1472-1482.

12 S. Zhang, F. Wang, J. Keats, X. Zhu, Y. Ning, S.D. Wardwell, L. Moran, Q.K. Mohemmad, R. Anjum, Y. Wang, N.I. Narasimhan, D. Dalgarno, W.C. Shakespeare, J.J. Miret, T. Clackson and V.M. Rivera, *Chem. Biol. Drug. Des.*, 2011, **78**(6), 999-1005.

13 T.H. Marsilje, W. Pei, B. Chen, W. Lu, T. Uno, Y. Jin, T. Jiang, S. Kim, N. Li, M. Warmuth, Y. Sarkisova, F. Sun, A. Steffy, A.C. Pferdekamper, A.G. Li, S.B. Joseph, Y. Kim, B. Liu, T. Tuntland, X. Cui, N.S. Gray, R. Steensma, Y. Wan, J. Jiang, G. Chopiuk, J. Li, W.P. Gordon, W. Richmond, K. Johnson, J. Chang, T. Groessl, Y. He, A. Phimister, A. Aycinena, C.C. Lee, B. Bursulaya, D.S. Karanewsky, H.M. Seidel, J.L. Harris and P. Michellys, *J. Med. Chem.*, 2013, **56**(14), 5675-5690.

14 S.I. Ou, M. Azada, D.J. Hsiang, J.M. Herman, T.S. Kain, C. Siwak-Tapp, C. Casey, J. He, S.M. Ali, S.J. Klempner and V.A. Miller, *J. Thorac. Oncol.*, 2014, **9**(4), 549-553.

15 W. Huang, S. Liu, D. Zou, M. Thomas, Y. Wang, T. Zhou, J. Romero, A. Kohlmann, F. Li, J. Qi, L. Cai, T.A. Dwight, Y. Xu, R. Xu, R. Dodd, A. Toms, L. Parillon, X. Lu, R. Anjum, S. Zhang, F. Wang, J. Keats, S.D. Wardwell, Y. Ning, Q. Xu, L.E. Moran, Q.K. Mohemmad, H.G. Jang, T. Clackson, N.I. Narasimhan, V.M. Rivera, X. Zhu, D. Dalgarno and W.C. Shakespeare, *J. Med. Chem.*, 2016, **59**(10), 4948-4964.

16 H.Y. Zou, L. Friboulet, D.P. Kodack, L.D. Engstrom, Q. Li, M. West, R.W. Tang, H. Wang, K. Tsaparikos, J. Wang, S. Timofeevski, R. Katayama, D.M. Dinh, H. Lam, J.L. Lam, S. Yamazaki, W. Hu, B. Patel, D. Bezwada, R.L. Frias, E. Lifshits, S. Mahmood, J.F. Gainor, T. Affolter, P.B. Lappin, H. Gukasyan, N. Lee, S. Deng, R.K. Jain, T.W. Johnson, A.T. Shaw, V.R. Fantin and T. Smeal, *Cancer Cell.*, 2015, **28**(1), 70-81.

17 A.Drilon, S.I. Ou, B.C. Cho, D. Kim, J. Lee, J.J. Lin, V.W. Zhu, M. Ahn, D.R. Camidge, J. Nguyen, D. Zhai, W. Deng, Z. Huang, E. Rogers, J. Liu, J. Whitten, J.K. Lim, S. Stopatschinskaja, D.M. Hyman, R.C. Doebele, J.J. Cui and A.T. Shaw, *Cancer Discov.*, 2018, **8**(10), 1227-1236.

18 L. Friboulet, N. Li, R. Katayama, C.C. Lee, J.F. Gainor, A.S. Crystal, P. Michellys, M.M. Awad, N. Yanagitani, S. Kim, A.C. Pferdekamper, J. Li, S. Kasibhatla, F. Sun, X. Sun, S. Hua, P. McNamara, S. Mahmood, E.L. Lockerman, N. Fujita, M. Nishio, J.L. Harris, A.T. Shaw and J.A. Engelman, *Cancer Discov.*, 2014, **4**(6), 662-673.

19 R.T. Bossi, M.B. Saccardo, E. Ardini, M. Menichincheri, L. Rusconi, P. Magnaghi, P. Orsini, N. Avanzi, A.L. Borgia, M. Nesi, T. Bandiera, G. Fogliatto and J.A. Bertrand, *Biochem.*, 2010, **49**(32), 6813-6825.

20 Z. Liu, J. Ai, X. Peng, Z. Song, K. Wu, J. Zhang, Q. Yao, Y. Chen, Y. Ji, Y. Yang, M. Geng and A. Zhang, *Acs. Med. Chem. Lett.*, 2014, **5**(4), 304-308.

21 Y. Wang, G. Zhang, G. Hu, Y. Bu, H. Lei, D. Zuo, M. Han, X. Zhai and P. Gong, *Eur. J. Med. Chem.*, 2016, **123**, 80-89.

22 L.Y. Xing, T.F. Jing, J.L. Zhang, M. Guo, X.Q. Miao, F. Jiang and X. Zhai, *Bioorg. Chem*., 2018, **81**, 689-699.
23 M. Guo, D.Y. Zuo, J.L. Zhang, L.Y. Xing, W.F. Gou, F. Jiang, N. Jiang, D.J. Zhang and X. Zhai, *Eur. J. Med. Chem.,* 2018, **158**, 322-333.
24 H.R. Lei, N. Jiang, X.Q. Miao, L.Y. Xing, M. Guo, Y. Liu, H.W. Xu, P. Gong, D.Y. Zuo and X. Zhai, *Eur. J. Med. Chem.*, 2019, **171**, 297-309.
25 M. Zheng, S. Luan, S. Gao, L. Cheng, B. Hao, J. Li, Y. Chen, X. Hou, L. Chen and H. Li, *Oncotarget*., 2017, **8**(24), 39143-39153.
26 L. Sun, C. Liang, S. Shirazian, Y. Zhou, T. Miller, J. Cui, J.Y. Fukuda, J. Chu, A. Nematalla, X. Wang, H. Chen, A. Sistla, T.C. Luu, F. Tang, J. Wei and C. Tang, *J. Med. Chem.*, 2003, **46**(7), 1116-1119.
27 S.I. Patiño-Camacho, M. Déciga-Campos, K. Beltránvillalobos, D.A. Castro-Vidalcd, R.M. Montiel-Ruize and F.J. Flores-Murrietaaf, *Eur. J. Pharmacol.*, 2017, **805**, 51-57.
28 E. Vitaku, D.T. Smith, J.T. Njardarson, *J. Med. Chem*., 2014, **57**(24), 10257-10274.
29 T.B. Sim, H.J. Yoon and W.Y. Hur. WO 2016006921, 2016.
30 Y.F. Zhao, M.Y. Jiang, S.G. Zhou, S.S. Wu, X.L. Zhang, L.S. Ma, K. Zhang and P. Gong, *Eur. J. Med. Chem.*, 2015, **96**, 369-380.
31 P. Leeson, *Nature.*, 2012, **481**(7382), 455-456.
32 M.T. Han, J.W. Shen, L.J. Wang, Y. Wang, X. Zhai, Y. Li, M.Q. Liu, Z.Q. Li, D.Y. Zuo and Y.L. Wu, *Chem. Biol. Interact.*, 2018, **284**, 24-31.
33 I.M. El-Deeb, B.S. Park, S.J. Jung, K.H. Yoo, C. Oh, S.J. Cho, D.K. Han, J.Y. Lee and S.H. Lee, *Bioorg. Med. Chem. Lett*., 2009, **19**(19), 5622-5626.

View Article Online
DOI: 10.1039/C9NJ05980F

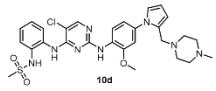

Cell	IC_{50} (μM)		Enzyme	IC_{50} (nM)	
	10d	ceritinib		10d	ceritinib
Karpas299	0.01	0.027	ALK	1.8	2.3
H2228	0.08	0.099	ALK^{L1196M}	4.3	8.9
HCC78	0.042	0.074	ROS1	3.6	2.7
H460	2.50	0.20	EGFR	>100	>100
A549	1.09	0.79